13th World Conference on Earthquake Engineering
Vancouver, B.C., Canada
August 1-6, 2004
Paper No. 112

NUMERICAL ANALYSES FOR THE SEISMIC SAFETY RETROFIT DESIGN OF THE IMMERSED-TUBE GEORGE MASSEY TUNNEL

Ernest NAESGAARD[1], Dan YANG[2], Peter BYRNE[3], and Blair GOHL[4]

SUMMARY

Dynamic numerical analyses were used for the seismic retrofit design of the 44-year-old immersed-tube George Massey Tunnel. The 1.3 km long tunnel carries four lanes of traffic under the Fraser River just south of Vancouver, British Columbia. Design criteria were that the retrofitted tunnel should withstand both a 0.25g magnitude 7.0 non-subduction earthquake and a 0.15g magnitude 8.2 distant subduction earthquake without collapse or loss of life, but with damage to a repairable level including controllable water leakage.

Soil liquefaction, its consequences, and mitigation were the key design challenges. Two-dimensional dynamic analyses using the program FLAC were the prime geotechnical analyses and design tool. Displacements from the numerical analyses were used as input into three-dimensional static structural analyses using non-linear soil springs and nonlinear moment-curvature section properties. The structural analyses were used to assess and mitigate potential cracking in the tunnel.

In the 2D FLAC analyses transverse and longitudinal sections were studied using total and effective stress constitutive models (UBCTOT and UBCSAND) developed at the University of British Columbia. Dynamic shaking, liquefaction triggering, consequences of liquefaction and soil-structure interaction were addressed in each of the models. Analyses were carried out with and without retrofit measures. A centrifuge-testing program was carried out to check the numerical model. There was good agreement between numerical and centrifuge test results. Field tests of seismic drains were also carried out.

Geotechnical retrofit measures proposed include: ground densification using vibro-replacement stone columns and drain columns on each side of the tunnel. Liquefaction was not mitigated below the tunnel and consequences of post-liquefaction settlement were allowed for in the geotechnical design. Other proposed structural and non-structural retrofit measures that include increasing structural reinforcement and adding new emergency pumps will further eliminate seismic vulnerabilities, in particular the consequences of post-liquefaction settlement, by ensuring more uniform ductility, crack and leakage control throughout the tunnel. The combined geotechnical and structural retrofit design will meet the required design criteria.

This paper focuses on geotechnical aspects of the design. Methodology and results of the numerical analyses and centrifuge testing are presented.

---

[1] Trow Associates Inc., Burnaby, B.C., [2] Buckland & Taylor Ltd., North Vancouver, B.C., [3] University of British Columbia, [4] Pacific Geodynamics Inc., Delta, B.C.

INTRODUCTION

A seismic upgrade design for the immersed tube George Massey Tunnel was completed in 2003. This paper describes the geotechnical aspects of the seismic upgrade design with emphasis on the numerical analyses methodology.

The George Massey Tunnel was built in 1958/59 as part of the highway 99 connecting Vancouver British Columbia with Washington State in US. The tunnel underlies the main channel of the Fraser River within the Fraser delta (Fig. 1). It is 1.3 km long, including a 370 m north approach, a 629 m immersed section, and a 335 m south approach. The immersed section has two shafts with two traffic lanes each plus two ventilation ducts located outside the roadway shafts (Fig. 2). It was pre-cast within a graving dock in 105 m long segments. The segments were floated to position and sunk within a shallow trench in the river bottom. Following sinking, voids under the tunnel were filled with washed-in sand. Rock fill was placed over the tunnel to counter buoyancy and scour. Approaches and ventilation towers were constructed within dewatered open cuts. The site conditions and construction of the tunnel is described by Hall [1]. A general description of the seismic upgrade is given by Yang [2].

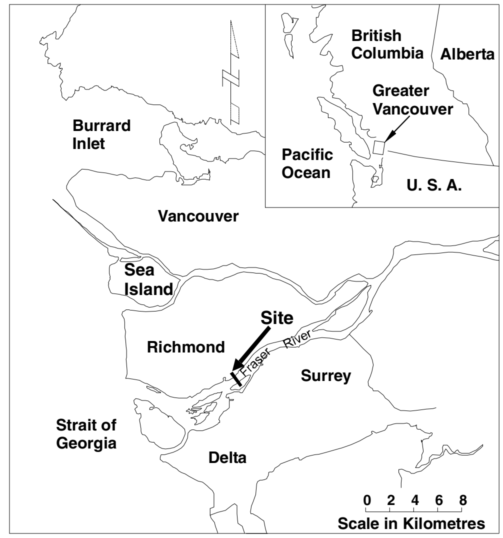

Figure 1 Location plan

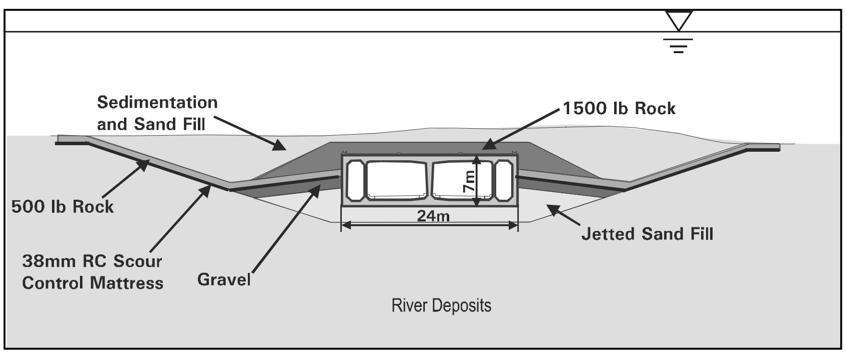

Figure 2 Section of immersed tunnel

The tunnel is a key part of the greater Vancouver infrastructure and it was imperative that the tunnel be retrofitted with minimum disruption to traffic.

DESIGN METHODOLOGY

The seismic upgrade design for the tunnel was conducted in two parts, (i) an initial seismic strategy design phase and (ii) a detailed design phase. During the strategy phase potential failure modes were reviewed and preliminary mitigation schemes, including a recommended scheme, were developed. During final design detailed analyses, drawings, and specifications for the work were developed. Centrifuge testing and full-scale testing of gravel drains were also carried out.

The basic geotechnical aspects of the seismic upgrade design included the following items:

- Review of available information and site history
- Establish design criteria
- Develop geological profiles, soil properties, and tunnel properties
- Develop potential modes of failure and mitigation

- Ground response analyses to develop design ground motion for use in dynamic analyses and liquefaction assessment
- Assessment of seismic wave passage and incoherence effects
- Preliminary analyses including:
    - Seed method liquefaction triggering assessment
    - Limit-equilibrium riverbank seismic stability with pre-liquefaction and post-liquefaction soil properties,
    - Limit-equilibrium tunnel flotation calculations with liquefied soil treated as a heavy liquid.
- Detailed dynamic numerical analyses
- Centrifuge tests for verification and calibration of numerical model
- Full-scale tests of gravel drains using sequential blasting to simulate earthquake shaking.
- Drawings and specifications.

SEISMIC DESIGN CRITERIA

Design criteria were that the tunnel should be retrofitted to withstand both a 0.25g magnitude 7.0 non-subduction earthquake and a 0.15g magnitude 8.2 distant subduction earthquake without collapse or loss of life and to restrict damage to a repairable level. Three non-subduction and one subduction time history records (Anderson [3]) were provided by the Ministry of Transportation, the owners of the tunnel. The non-subduction records had been fitted to the Geological Survey of Canada Uniform Hazard spectrum (Adams [4]) that has a 10% probability of being exceeded in 50 years or a return period of 475 years. The subduction record had been fitted to a spectrum derived using Young's [5] attenuation relationship with a distance of 120 km and magnitude of 8.2. Outcropping firm ground (very dense Pleistocene soil or soft rock) spectrum for the non-subduction and subduction design earthquakes are shown in Fig. 3.

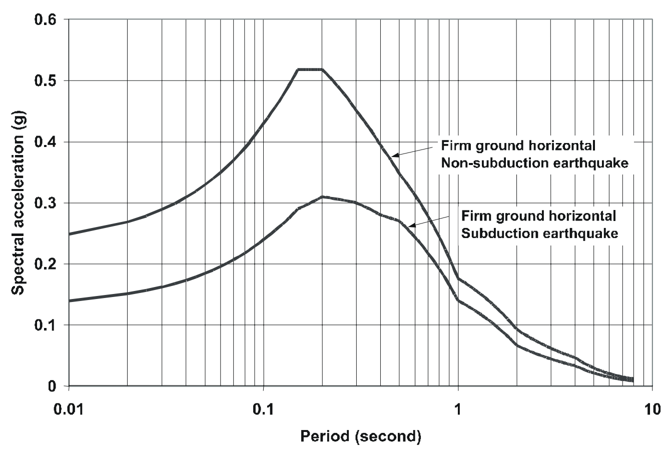

Figure 3 Firm ground design spectra for 5% damping

GEOLOGICAL AND HYDROLOGICAL SETTING

The tunnel is located within the Fraser River delta under the main arm of the Fraser River approximately 15 km from the delta's immergence from the uplands and 9 km upstream from the river's mouth (Fig. 1). The Fraser River delta evolved in the Holocene following retreat of the glaciers approximately 10,000 years ago. With retreat of glacial ice, a thin layer of glaciomarine pebbly silts was deposited followed by bottomset marine silt and clay sediments up to about 120m thickness (Monahan [6]). These marine sediments would be similar to the modern Strait of Georgia sediments. Then, as the delta prograded west, these marine deposits are overlain by foreset delta-front deposits. These are coarser than the bottomset deposits and consist of silts interlayered with fine silty sand. With advancement of the delta, the marine and delta front clays and silts were overlain by topset fluvial sands (Fraser River Sand). These sands are often cross-bedded, relatively uniform, of medium grain size, and very loose to medium dense. Prior to development, the river channel would migrate back and forth across the delta with infill on one side of the channel and erosion on the other. Occasionally channels would be abandoned and form sloughs that would be in-filled with silt in lieu of sand. Adjacent to the river channels, the fluvial sands are covered with flood plain and delta front silts. In recent times (approx. last 100 years) the location of the river has been controlled by dredging, dykes, and rip rap armour. The ground profile at the tunnel site is summarized in Table 1.

Table 1 Geological profile at tunnel site

Description	Geologic Age (years ago)	Depth to top of deposit (m)		SPT $(N_1)_{60}$ (blows/ft) [Shear Wave Velocity (V'_s) (m/s)]	Reference
		River bank	River channel		
Fill (typically river sand)	0 to 100	0	N/A	5 to 30 [50 to 150]	Gillespie[7] & CANLEX[8]
Floodplain silts	Holocene (0 to 2K)	0 to 4	N/A	2 to 8 [60 to 120]	"
Fluvial River Sands	Holocene (0 to 2K)	3 to 5	0	5 to 25 [80 to 200]	"
Marine Sediments	Holocene (1K to 13K)	20 to 32	7 to 20	3 to 20 [150 to 350]	"
Glacial deposits	Pleistocene (10K to 50K)	Approx. 300		[450 to 760]	McGee[9] & Britton [10]
Sedimentary bedrock	Tertiary (50M)	Approx. 600 to 700		[700 to 1800]	Britton [10] & Hunter [11]

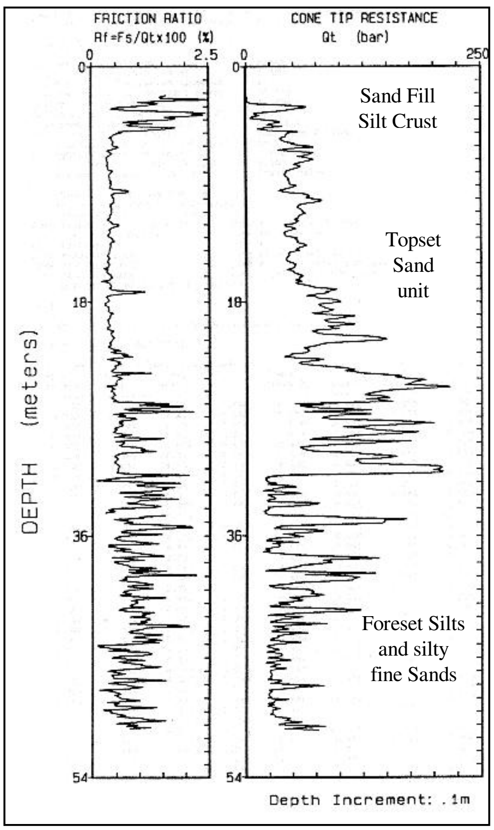

Figure 4 Typical cone penetration test on flood plain adjacent to south approach (CANLEX [8])

Drilling for the tunnel was conducted at the time of the original construction in 1957 and by the Ministry of Transportation in 1991 (Gillespie [7]). Detailed site investigation and laboratory testing was also carried out just north of the south approach as part of the CANLEX research project (CANLEX [8]) in 1993/4. A typical cone penetration test profile is shown in Fig. 4. A cross-section as interpreted from available boreholes is shown in Fig. 5.

The flow in the main arm of the Fraser River varies from about 500 m^3/s to 12,000 m^3/s with peaks coinciding with snowmelt in the mountains in late spring and early summer (Morrison [12], Monahan [6]). The river is a shipping channel and is periodically dredged to maintain the channel depth and has dykes to prevent adjacent lands from flooding. The upper 10 to 15 m of the sand in the river channel is mobile and subject to scour, especially during the spring freshet. This results in depressions in the river bottom that vary in size and location with time (Fig. 6). At the tunnel site the river is tidal. This causes hourly changes in flow velocity and river water levels. The tidal range is about 3m, however the elevations varies with time of year and river flow. The water in the lower portions of the river is often brackish.

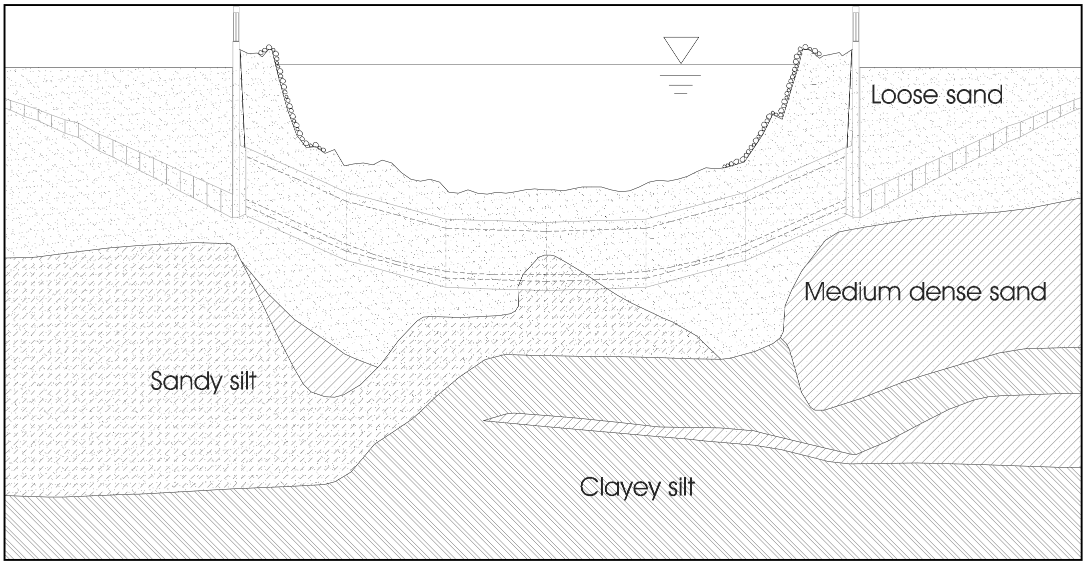

Figure 5 Cross-section as interpreted from available testholes (not to scale – section shown is approximately 50 m deep and 1000 m wide)

POTENTIAL TUNNEL VULNERABILITIES & MITIGATION SCHEMES

Potential tunnel vulnerabilities

The following potential vulnerabilities were considered:

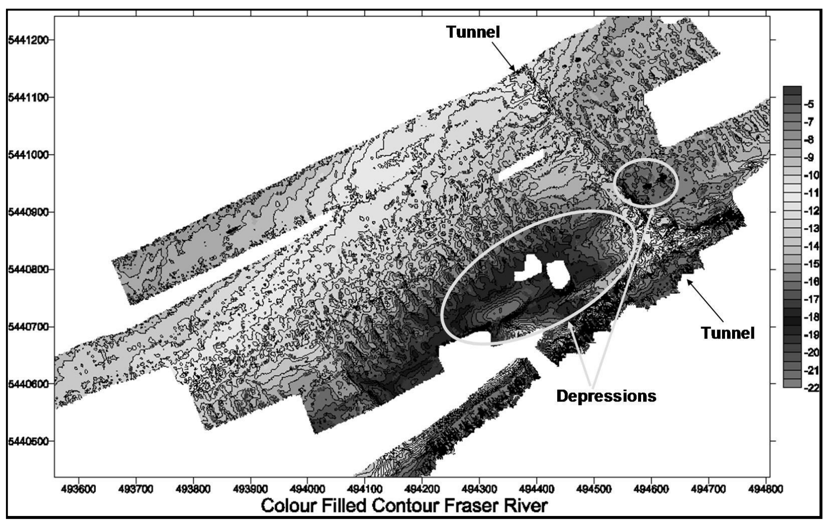

Figure 6 River bottom contours showing local depressions

- Wave passage effects – The tunnel is relatively long and seismic motions will vary along its length. Compression, shear, and surface waves will induce stresses in the tunnel as they travel along the tunnel length. Variation in the soil column along the length of the tunnel will also result in additional variation of ground motion along the tunnel.
- Soil liquefaction effects – liquefaction results in drastic reduction in soil strength and stiffness that can result in soil failure and differential displacements in the tunnel. This:
  - May cause flotation of the tunnel (reverse bearing failure) due to the tunnel being lighter than the adjacent soil,
  - May result in transverse movement of soil in the river if the river bed is not level,
  - May result in failure or movement of soil from the river banks toward centre channel,
  - May result in upward heave of the approach structures,

    - May result in differential consolidation settlements due to post-liquefaction dissipation of pore pressures
- Groundwater migration effects - High groundwater pore pressures generated by earthquake shaking can:
    - Migrate vertically to form potential water interlayer with limited or no strength,
    - Migrate laterally under the tunnel or approach structures and push them upwards
- Dyke failure and inflow of water within approaches
- Other non-geotechnical items – structural inadequacies; inadequate pump capacity; and inadequate emergency power

Potential mitigation schemes

Alternative seismic retrofit schemes for the tunnel were reviewed. Some of the items considered include:

- Sheet piles adjacent to tunnel to stop liquefied soil and water from moving in under tunnel,
- Compaction grouting under and adjacent to tunnel to control post-liquefaction settlements,
- Jet-grouting beside tunnel to prevent soil movement under tunnel and to support the tunnel,
- Supporting tunnel with mini-piles or pipe piles to minimize post-liquefaction settlement,
- Densification on either side of tunnel (vibro-replacement; timber compaction piles; gravel compaction piles; compaction grouting),
- Installation of seismic drains adjacent to tunnel or under tunnel, and
- Other items: Structural, emergency pump, and standby power upgrades.

GROUND RESPONSE ANALYSES

The design earthquake motions provided were for outcropping firm ground. At this site the firm ground is at approximately 300 m depth, whereas the tunnel is near the ground surface. Extending the 2D numerical models to 300m depth would have made the models prohibitively large and slow. A ground response analyses was carried out using the program SHAKE91 (Idriss [13]) in order to obtain: time histories at 50m depth to input into the 2D numerical analyses, and cyclic stress ratio for preliminary liquefaction triggering assessment. Six soil profiles with variation in the upper 50 m were analyzed. Time histories for numerical analyses were baseline corrected and filtered of motion with frequencies higher than 12 hz in order to be compatible with grid dimensions.

GROUND MOTION INCOHERENCE CONSIDERATIONS

Incoherence of ground motion was accounted for by considering wave passage effects, soil column effects, and differential liquefaction effects. Wave passage effects assuming a wave travelling in underlying rock at 2000m/s gave differential displacements of less than 50mm over 650m of tunnel. Soil column effects from different ground profiles in the upper 50m gave additional differential settlements in the order of 20mm. Differential movements due to soil liquefaction resulted in movements over an order of magnitude greater and were the controlling design consideration.

PRELIMINARY ANALYSES

Previous studies - Previous preliminary studies by Gillespie [7], Puar [14], and Hardy BBT [15] were reviewed.

Liquefaction assessment - Preliminary liquefaction assessment was conducted using the procedures by Robertson [16] and Fear [17], cyclic stress ratio (CSR) from ground response SHAKE91 analyses, and Q_t

from the CPT holes. These analyses indicated that the loose sands surrounding the tunnel are liquefiable during the design earthquake.

Tunnel flotation - Force-equilibrium stability analyses with the tunnel surrounded by liquefied soil modelled as a heavy liquid with no shear strength gave a factor of safety less than 1.0 against tunnel flotation. The same analysis with existing static conditions without soil liquefaction gave a factor of safety of 1.25.

Riverbank stability - Limit equilibrium slope stability analyses of the riverbanks gave pre-liquefaction factor of safety of 1.6 and a factor of safety less than 1.0 when liquefied soil with residual shear strength of 5 to 20 kPa was used.

DYNAMIC NUMERICAL ANALYSES

Dynamic analyses of the soil / tunnel system were carried out to provide insight into its behaviour during the design earthquake. The commercially available program FLAC (Itasca, [18]) with constitutive models, developed at University of British Columbia specifically for modeling the dynamic behaviour of liquefiable sands, were used for the analyses. FLAC is a two dimensional explicit finite difference numerical program developed for analyzing rock, soil and rock/soil/structure systems. Dynamic analyses are conducted in the time domain with very small time steps. Inertial forces are included in the equations of equilibrium solved during each step making the program well suited for analyzing partially stable or unstable systems. Both a total stress constitutive model (UBCTOT) (Beaty [19] & [20]) and an effective stress constitutive model (UBCSAND) (Puebla [21], Beaty [22], Byrne [23]) were used for the Massey Tunnel analyses.

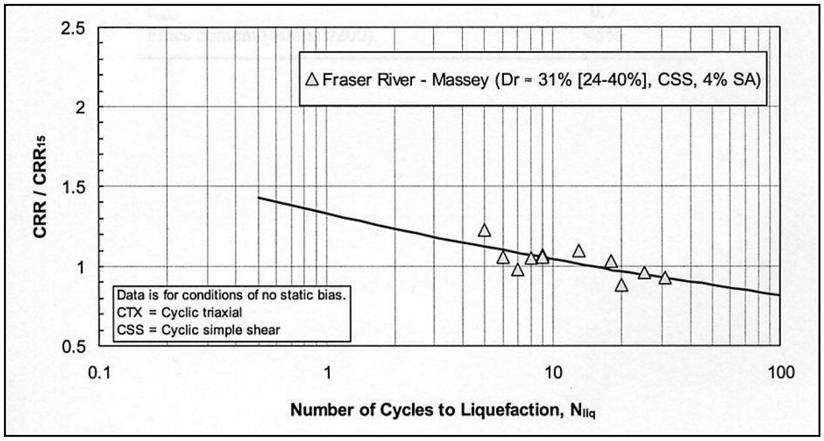

Figure 7 CRR/CRR15 for Fraser River Sand (from Beaty [19])

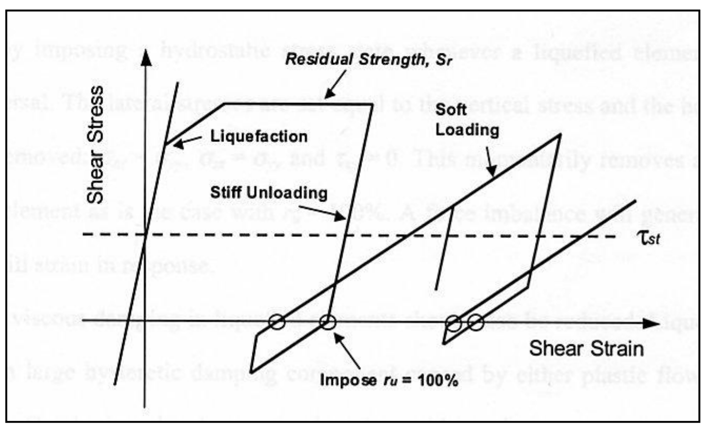

Figure 8 Bilinear stress strain behaviour of liquefied sand (from Beaty [19])

UBCTOT total stress synthesized model

This model tracks the dynamic shear stress history within each element and if a specified threshold is reached it changes the soil element properties to post-liquefaction values. The FLAC Mohr Coulomb model with equivalent linear shear modulus (G) and undrained bulk modulus (K) are used prior to liquefaction triggering. However, during the dynamic analysis the model tracks the dynamic cyclic shear stress history τ_{cyc} within each element, where $\tau_{cyc} = \left| \tau_{st} - \tau_{xy} \right|$, τ_{st} equals the static shear prior to dynamic excitation and τ_{xy} is the shear stress on the horizontal plane. The irregular shear stress history caused by the earthquake is interpreted as a succession of half cycles. Each half cycle of cyclic shear stress is transformed into an equivalent number of cycles N_{eq} at τ_{15}, where τ_{15} is the cyclic shear stress required to cause liquefaction in 15 cycles. If the threshold is reached ($\Sigma N_{eq} \geq 15$) then liquefaction is triggered in the element by changing the soil properties to the post-liquefaction values. Figure 7 shows the weighting curve used to establish the correlation between τ_{cyc} and N_{eq}. Figure 8 illustrates the stress strain response used with the UBCTOT model before and following liquefaction. Table 2 summarizes soil properties used in both the total and effective stress models. Raleigh damping of 4 to 8% was used with the total stress model.

The total stress dynamic analyses involved the following sequence:

- Establish the grid geometry,
- Establish elastic soil & structure properties, initial stresses and solve for static equilibrium,
- Calculate and input Mohr Coulomb soil properties, establish water table, pore water pressures and solve for static equilibrium,
- Change to undrained soil properties and solve for static equilibrium,
- Initiate dynamic analyses by changing to the UBCTOT constitutive model in potentially liquefiable elements, by applying 'free-field' boundaries to ends of model grid and by applying an earthquake time history to the base of the grid,
- During the dynamic analysis the total stress liquefaction triggering model (UBCTOT) evaluates triggering of liquefaction by tracking the dynamic shear stress history within each element. If the threshold is reached ($\Sigma N_{eq} \geq 15$) then liquefaction is triggered in the element by changing the soil properties to the post-liquefaction values.
- The analyses are continued to the end of the earthquake time history.
- Following dynamic analysis post-liquefaction consolidation settlements were estimated from the extent of liquefaction and $(N_1)_{60}$ using the procedures by Tokimatsu [24].

UBCSAND effective stress model

UBCSAND is an elastoplastic effective stress model with the mechanical behaviour of the sand skeleton and pore water flow fully coupled. The model includes a yield surface related to the developed friction angle, non-associative flow rule (Figure 9), and definitions for loading, unloading, and hardening. A hyperbolic relationship is used between stress ratio and plastic shear strain (Figure 10). Model parameters have been approximated from published data and model calibrations with laboratory simple shear tests. Soil properties used are given on Table 2. Key elastic and plastic parameters used in the Massey Tunnel analyses were derived in terms of normalized standard penetration test values, $(N_1)_{60}$ that were adjusted so as to give a good match with simple shear laboratory tests. 2% Raleigh damping was used with the UBCSAND model.

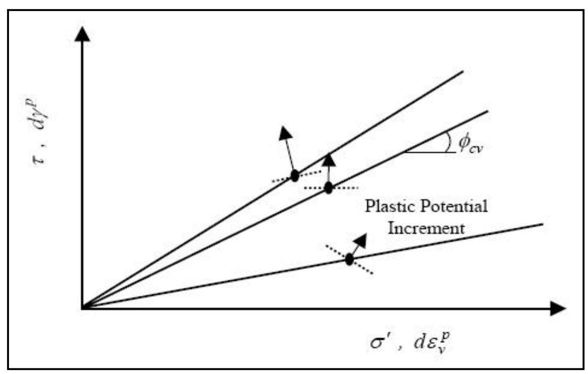

Figure 9 Non-associated flow criteria in UBCSAND

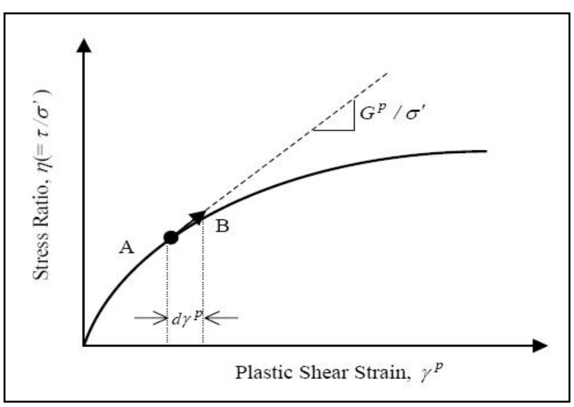

Figure 10 Hyperbolic relationship between stress ratio and plastic shear strain

The effective stress dynamic analyses involved the following sequence:

- Establish the grid geometry (used same grid as total stress analysis)
- Calculate elastic soil properties and solve for

static equilibrium,

- Calculate and input Mohr Coulomb drained soil properties, pore water pressures and solve for static equilibrium using a low fluid modulus,
- Change to UBCSAND model within granular soils,
- Turn fluid flow on and increase fluid modulus (used $5x10^5$kPa) and bring to static equilibrium
- Initiate dynamic analyses by applying 'free-field' boundaries to ends of model grid and by applying an earthquake time history to the base of the grid,
- During the dynamic analysis the pore pressures are generated by shear induced plastic volume change. This reduces mean effective stress and initiates pore water flow from zones of high head to low head.
- The analyses are continued to the end of the earthquake time history.
- Following dynamic analysis post-liquefaction consolidation settlements are estimated from the extent of liquefaction and $(N_1)_{60}$ using the procedures by Tokimatsu [24]. An alternative to independent calculation of post-liquefaction settlement was to continue the analysis past the end of earthquake shaking. The dissipation of excess pore pressures then results in consolidation settlements. However this process is time consuming. The version of UBCSAND used for the work also underestimated post-liquefaction consolidation and a change in modulus was required to achieve settlements similar to that calculated using the procedures by Tokimatsu [24].

Table 2 Soil properties used in both total and effective stress analyses

Soil parameters for all analyses	Native sand	Native silt	Rock & gravel fill	Sand fill over tunnel	Jetted sand fill
Density (kg/m^3)	1885	1784	2000	1850	1850
SPT $(N_1)_{60}$ (blows/300mm)	2 to15[a]	-	25	10	5 to 6
Cohesion (Pa)	-	$8x10^4$ to$1.0x10^5$	-	-	-
Parameters for effective stress analysis					
Permeability (cm/s)	$1x10^{-3}$ to $2x10^{-4}$	$1x10^{-5}$	$1x10^{-3}$	$1x10^{-3}$	$1x10^{-3}$
Porosity	0.45 to 0.47	0.51	0.4	0.47	0.47
Peak friction angle, ϕ_f (^{o})	34	-	45	34	34
Constant volume friction angle, ϕ_{cv} (^{o})	33	-	33	33	33
Elastic and plastic shear modulus number, k_G^e and k_G^p	Functions of $(N_1)_{60}$				
Elastic bulk modulus number, k_B^e	Function of $(N_1)_{60}$				
Parameters for total stress analysis					
Internal friction angle, ϕ (^{o})	34	-	45	34	34
Elastic bulk modulus, B (Pa)	$3\text{-}6.5x10^7$	$1.4\text{-}1.7x10^8$	$2.7x10^7$	$1.3x10^7$	$1.0x10^7$
Shear modulus at small strain, G_{max} (Pa) (Beaty[19])	$440*(N_1)_{60}^{1/3}*P_a*(\sigma'_m/P_a)^{1/2}$ where P_a = atmospheric pressure, σ'_m = mean effective stress				
B/G_{dyn} (where G_{dyn} = equivalent shear modulus of nonliquefied soil during cyclic loading)	10.0 for saturated, non-liquefied elements				
B/G_{liq} (where G_{liq} = post-liquefaction shear modulus during loading)	50.0 for saturated, liquefied elements				
Mobilized residual strength, S_r (Pa) (Beaty[18])	$\sigma'_{vo}*0.025*e^{0.16*(N1)60}$ where σ'_{vo} = initial vertical effective stress				
Residual shear strain, γ_r	S_r/G_{liq}				

[a] $(N_1)_{60}$ of native sand was randomly varied with a mean of 6 and a coefficient of variation of 30%.

Grid configurations
The size of grid elements was controlled by wave propagation-frequency considerations. Free-field boundaries were used for opposite ends of the mesh. The FLAC free-field boundaries did not appear to be compatible with drastic changes in soil properties that occur when the soil liquefies. To overcome this, end elements were kept elastic and the end boundaries were kept well away from areas of interest. When opposite mesh ends were the same height and soil type then opposite ends of the grid were attached in lieu of using free-field boundaries. The river water was modelled as an applied pressure to the top of the mesh. This pressure was updated periodically during the dynamic analyses in order for the applied pressure to be compatible with grid deformations.

Transverse and longitudinally aligned grids were developed. The transverse section was used to assess the effects of liquefaction around the tunnel, effects of undulations in the riverbed, effects of pore pressure and groundwater redistribution, and to design and optimize remedial measures.

The proposed remediation measures (densification and drains) are all on the sides of the tunnel and do not prevent liquefaction below the tunnel. There was concern that liquefied soil or water under the tunnel may flow longitudinally under the tunnel from the higher stressed zone under the river banks toward the lower stressed zone within the river channel. This would result in settlement of the river banks and heave of the tunnel within the river channel. The longitudinal model was developed to assess this migration effect.

Transverse model
2D Transverse dynamic analyses were conducted with both the total stress and effective stress models. Figure 11 shows typical transverse grid. The cross-sectional area and density of the structural elements used to model the tunnel was adjusted to give the tunnel structure the correct average density. Analyses were carried out:

- With various earthquake motions
- With horizontal and sloped river bed
- With various soil profiles and material properties
- With alternative remediation measures including: ground densification, sheetpiles, and gravel drains. Various widths of densification were modelled as part of optimizing the design.

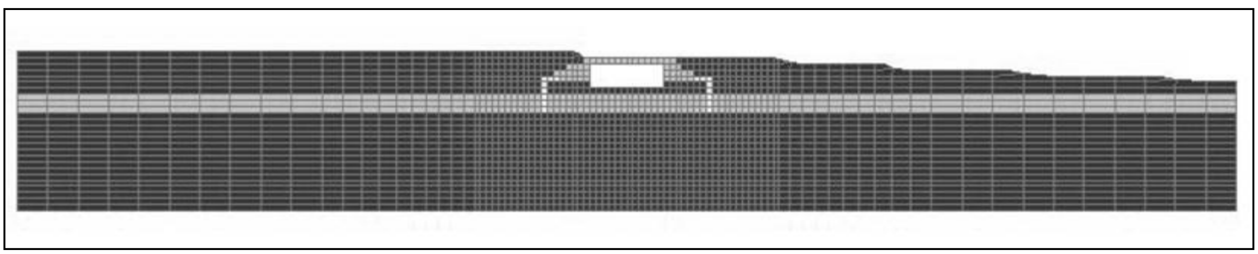

Figure 11 Typical transverse grid with slope in river bottom on right side (grid is 52m deep by 400m wide)

Longitudinal model
Figure 12 illustrates the typical longitudinal model. The model is 32 elements high by 311 elements wide for a total of approximately 10,000 elements. The model is approximately symmetrical about the river channel and includes the immersed tunnel and both approaches. The tunnel structure was modelled with a single beam element with the stiffness and yield moment similar to the tunnel section. Soil surrounding the beam element within the area of the tunnel was modelled with a density equivalent to the average density of the tunnel. Incoherence (wave travel) effects were modelled by placing delays to the time history so that the input travelled from one end of the model to the other at approximately the speed of the

shear wave in the basement bedrock. Vertical input motion was also applied in some analyses. It was taken as 2/3 of the horizontal firm ground motion at 300m depth.

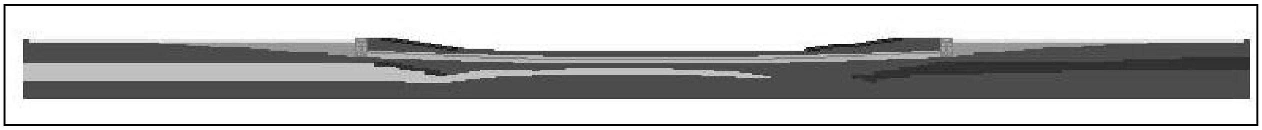

Figure 12 Longitudinal model showing various soil zones (model is 60m high by 1345m wide)

Following completion of the dynamic analysis the liquefied elements were allowed to consolidate. For the total stress model this was accomplished by applying increments of vertical stress until the correct volumetric strain had occurred. The correct volumetric strain was calculated using the procedures by Tokimatsu [23]. In the effective stress model the volumetric strain occurred automatically by allowing the pore water pressures to dissipate to hydrostatic values. Adjustments had to be made to the post-liquefaction bulk modulus in order for the volumetric strains to match the values obtained using the procedure by Tokimatsu [23].

Results of dynamic analyses

The following are some of the key observations from the numerical analyses:

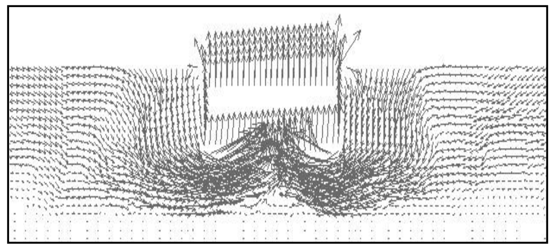

Figure 13 Upward flotation or reverse bearing failure of tunnel when surrounding soil liquefies

- With *level river bottom* and *no ground improvement* the tunnel will heave in the range of 0.5 to 1.5m following soil liquefaction (Fig. 13). The bulk of the movement occurs during strong shaking following liquefaction, but minor movements may continue to the end of the earthquake and longer.
- With a *sloping river bottom* and *no ground improvement* the tunnel heaves less (0.2 to 0.3m), but moves laterally significantly in the range of 1 to 2m (Fig.14).

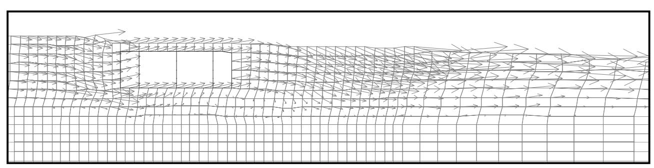

Figure 14 Displacement vectors & displaced grid with sloping river channel

- If *horizontal impervious silt layers* with large lateral extent are present within the liquefiable sand unit then a slow ongoing heave of the tunnel may continue long after the end of earthquake shaking. This movement is additional to the movement that occurs during earthquake shaking and is due to high pressure groundwater generated by liquefaction in soil adjacent to the tunnel seeping under the tunnel and pushing it up. This movement could continue for many minutes or hours after the end of earthquake shaking. Installation of drainage columns within the proposed densified ground reduces this ongoing movement significantly.
- Sheet piles with large sectional modulus were effective in reducing movement of soil under the tunnel and related tunnel heave. However the sheet piles were more costly than alternative measures. They are also more flexible than the densified ground, therefore not efficient at reducing lateral movements if the river bed sloped.
- During initial strong shaking the tunnel experiences both compression and tensile stresses, however, with the onset of liquefaction the central river section of the tunnel has a net

compressive stress. Lateral movements of the tunnel due to slope in the river bottom and due to differential settlement will give local bending stresses within the tunnel.

- Incoherence (traveling wave effects) and vertical input motion did not have a significant influence on tunnel response compared to the effects of ground liquefaction.

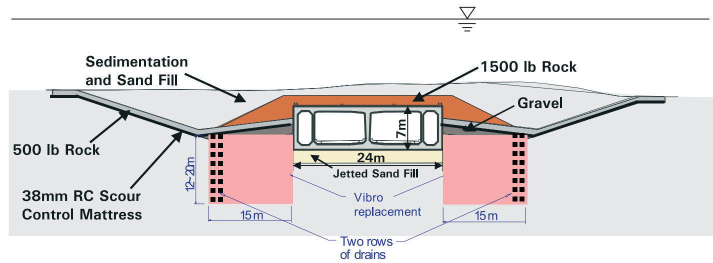

Figure 15 Final remediation scheme with ground densification and drainage

- The total stress model (UBCTOT) and effective stress model (UBCSAND) gave similar displacements during the period of dynamic shaking. However, only the effective stress model could emulate pore pressure migration effects (that could result in tunnel heave after the end of earthquake shaking).
- Based on the numerical analyses with the proposed *final design remediation scheme*, the lateral movements of the tunnel should be less than 0.1 to 0.4m. Vertical heave should be less than 0.2m and differential settlement due to post-liquefaction consolidation should be less than 0.6m over a length of 250m. This includes movements during and following earthquake shaking.

Recommendations for final design for the tunnel are illustrated on Fig. 15. The design includes a 15 to 20 m width of vibro-replacement densification on either side of the tunnel with the outer two rows of columns designed to act as drains by being constructed with 2 to 5 mm diameter filter (drainage) gravel. Densification was not deemed necessary adjacent to the approaches. However, one to two rows of seismic drains on 2m centres were specified to assist in relieving high pore pressures. The on-land seismic drains are to be at least 200mm in diameter and include a slotted pipe surrounded with 2 to 5 mm diameter drainage gravel.

CENTRIFUGE TESTING FOR NUMERICAL MODEL VERICFICATION

Centrifuge testing was carried out in order to validate and calibrate the numerical models. Details on the centrifuge tests are given in Yang [2], and Adalier [25] and only a summary is given here. Three tests were carried out at Rensselaer Polytechnic Institute (RPI), NY, USA in 2002. The tests were designed to model a transverse section of the tunnel. The first test (Model #1) was with no ground improvement adjacent to the tunnel, the second (Model #2) was with 10 m of densification on either side of the tunnel, and the third (Model #3) was with a 10 m drainage zone on either side of the tunnel. Fig. 16 shows the layout of the second test and the location of the instrumentation. The layout for the other two tests was similar. The tests were run at 100g. Nevada sand, with a permeability approximately 1/4 that of Fraser River sand and a methylcellulose pore fluid with a viscosity of 25 times that of water, was used for the tests. This combination resulted in scaling of 100:1 giving prototype dimensions, stresses and flow characteristics similar to that which would occur if the tunnel was surrounded with Fraser River sand. The whole model was inclined at a two degree slope in order to emulate some unevenness in the river bottom.

Class A predictions of the centrifuge tests were made prior to the tests being conducted. Table 3 summarizes displacements and accelerations of the predictions and tests. The numerical model and test results were in close agreement. Typical displacement, pore pressure and acceleration time histories from the effective stress numerical analyses and centrifuge tests are compared in Figures 17, 18, and 19.

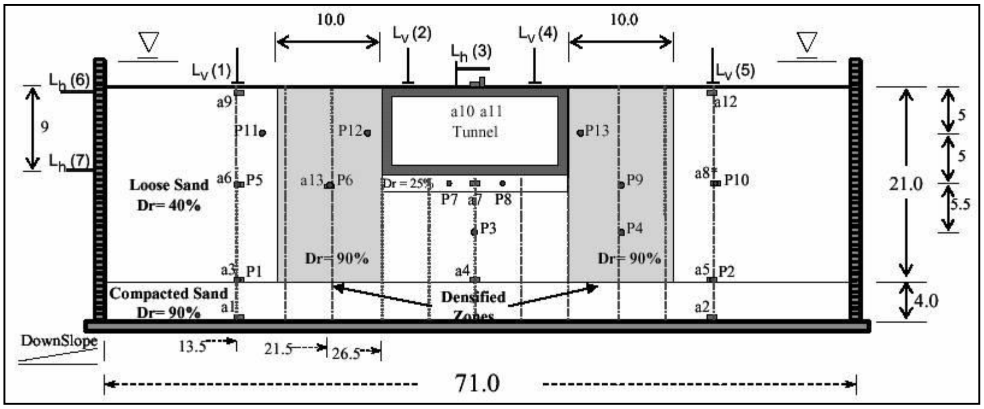

Figure 16 Model 2 centrifuge test layout (Legend: a3 = accelerometer; P12 = piezometer; Lv & Lh= LVDT) . Dimensions in centimeters. Model 1 and Model 3 similar.

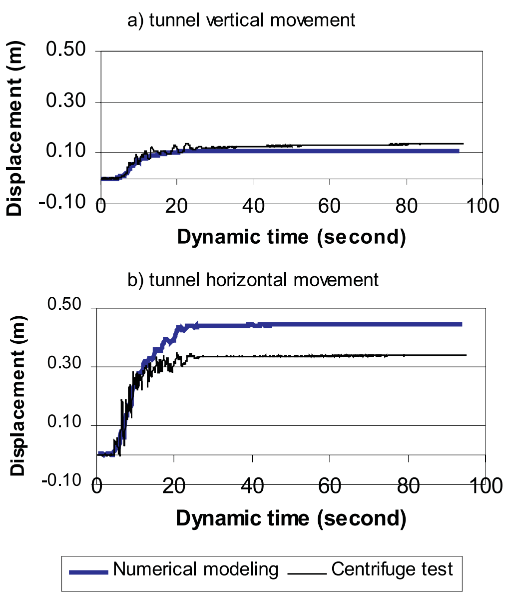

Figure 17 Comparison of numerical and centrifuge results for Model #2 with 10m wide densification

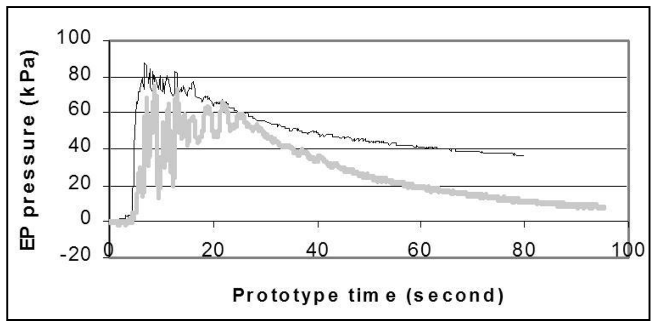

Figure 18 Comparison of pore pressure in piezometer P5 in Model #3 (dark colour is FLAC output and lighter colour is centrifuge test result)

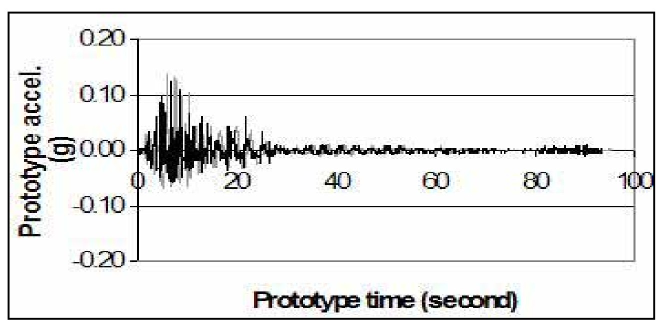

Figure 19 Model #1 accelerometer A10 (dark line is FLAC & light line is from centrifuge test)

Table 3. "Class A" numerical predictions compared to centrifuge test results (in prototype scale)

Output parameter	Scaling factor (model:prototype)	Model 1(1)	Model 2(2)	Model 3(3)
Peak tunnel heave (m)	1:100	0.25 (0.27)	0.13 (0.14)	0.12 (0.04)
Peak tunnel lateral movement (m)	1:100	0.59 (0.68)	0.50 (0.35)	0.40 (0.30)
Maximum soil displacement (m)	1:100	1.52 (1.50)	1.20 (1.30)	1.03 (1.10)
Peak tunnel horizontal acceleration (g)	100:1	0.10 (0.11)	0.13 (0.08)	0.095 (0.095)

Note: Numbers given in brackets are the results from the centrifuge tests.

(1) No ground improvement – loose sand around tunnel
(2) 10m wide densification on each side of tunnel
(3) 10m wide drainage zone on each side of tunnel

GRAVEL DRAIN TEST PROGRAM

Field testing of gravel drains using sequential blasting to trigger ground liquefaction was carried out. Two tests were carried out. One test area had no seismic drains, and the other had three seismic drains. The efficiency of different drain backfill materials (fine gravel and coarse sand) and the effects of central slotted pipe diameters were examined. Flows from the gravel drains and pore pressures around the drains were measured. The field test results showed:

- Large groundwater flows created by blast-induced liquefaction were discharged by the gravel drains over several minutes following the blast. A total volume of flow of 2300 liters was handled by the gravel drain constructed using a gravel backfill and the largest (75mm ID) central slotted pipe. Smaller volumes of flow were handled by the drains containing smaller diameter pipes and/or the use of a coarse sand backfill.
- The drain with the coarse sand backfill which satisfied accepted filter criteria ran cleaner than the drains with the fine gravel filter.
- The three drains flowed following a later nearby blast (conducted for a test by others), indicating that they were functional for more than one liquefaction event.
- The three drains did not prevent liquefaction from occurring, nor did they significantly accelerate pore pressure dissipation within the test area (compared to that without drains). A greater density of drains may be required to provide effective pore pressure relief.

A numerical simulation using the UBCSAND effective stress model and FLAC was also carried out to calibrate the modelling of the gravel drains (Yang [2]).

CONCLUSIONS

Dynamic numerical analyses were a key tool for identifying the seismic vulnerabilities of this immersed-tube concrete tunnel and in implementing structural retrofit and ground improvement strategies. The analyses gave insight into the behaviour of the liquefied soil/tunnel system and allowed the performance of various mitigation measures to be assessed and optimized. The final geotechnical retrofit scheme was selected based on levels of tunnel movement assessed to be acceptable by the structure. The variability and uncertainty of soil conditions were considered and cost comparisons of different ground retrofit schemes were carried out.

The effective stress and total stress constitutive models used gave similar ground displacements at the end of the earthquake. However, only the effective stress model is able to emulate the migration of pore water that may cause potential post-earthquake heave movements.

Centrifuge testing of the tunnel model without retrofit, with densification retrofit and with drainage retrofit was part of the design process. These tests verified tunnel failure modes and the ability of the numerical models to predict the behaviour. A better match between the numerical data and centrifuge data was achieved when stress densification effects (Park [26]) from the centrifuge spin-up were considered.

Field gravel drain testing using sequential blasting to liquefy the ground showed that the drains were effective in discharging large flows of water. The tests were not conclusive in assessing the effectiveness of the three drains in accelerating pore pressure dissipation rates. A larger number of drains would be needed to achieve higher pore pressure dissipation rate.

The final geotechnical retrofit design including both ground densification and seismic drains was selected based on the optimisation study conducted by the numerical models.

ACKNOWLEGEMENTS

The writers wish to thank Mr. William Szto and Dr. Don Gillespie from the Ministry of Transportation of B.C. (MOT) for permission to publish this paper and their coordination and technical contribution during the project. The writers thank the project manager Dr. Peter Taylor, the senior structural engineer Dr. Hisham Ibrahim of Buckland & Taylor Ltd. and the peer reviewers Prof. Don Anderson and Prof. Peter Byrne (also a co-author) of University of British Columbia for their technical assistance and special contributions to the work. Special thanks go to Dr. Korhan Adalier, Dr. Tarek Abdoun, Dr. Ricardo Dobry of RPI and Dr. Ryan Phillips of C-CORE, who conducted successful centrifuge tests for the project. The design team included Buckland & Taylor Ltd. (Prime Consultant), Trow Associates Inc., Pacific Geodynamics Inc., Ben C. Gerwick Inc., AMEC, Levelton Engineering, Dr. W. Tseng and Dr. M. Collins.

REFERENCES

1. Hall, P., Broendum-Nielsen, T., and Kivisild, H.R. 1957. Deas Island Tunnel. Journal of the Structural Division, ASCE, 83(ST6), November, 1957
2. Yang, D., Naesgaard, E., and Gohl, B. “Geotechnical seismic retrofit design of George Massey Tunnel.” In Proceedings of 12th Pan-American Conference on Soil Mechanics and Geotechnical Engineering, Cambridge, USA, June 22-26, 2003, pp. 2567 – 2574.
3. Anderson, D., Cherry Nathan Anderson, Report to Ministry of Transportation & Highways.
4. Adams, J., Weichert, D.H., and Halchuk, S., "Trial seismic hazard maps of Canada - 1999: 2%/50 year values for selected Canadian cities". Geological Survey of Canada Open File 3724, 100 pp., 1999.
5. Youngs, R.R., Chiou, J.-J., Silva, W.J., and Humphrey, J.R. “Strong ground motion relationships for subduction zone earthquakes.” Seismological Research Letters, v. 68, 1997, p.58-73.
6. Monahan, P.A., Byrne, P.M, Watts, B.D. and Naesgaard, E., “Engineering geology and natural hazards of the Fraser River Delta,” in Guidebook for Geological Field Trips in Southwestern British Columbia and Northern Washington, Geological Association of Canada Cordilleran Section, Edited by Woodsworth, Jackson, Nelson and Ward, April, 2000, pp. 27-47.
7. Gillespie, D., “Massey Tunnel Site Investigation”, Ministry of Transportation & Highways, British Columbia, June, 1991
8. CANLEX, “General Site Characterization, Massey Tunnel.” Report prepared for CANLEX project by University of British Columbia, Phase II, Activity 3A, January1995.
9. McGee, T.M., Hunter, J.A., Spence, R.A., & Luternauer, J.L., “Mapping the Shallowest Surface of More Compact Sediments Predating Fraser River Deltaic Deposits., 1998.

10. Britton, J.R., Harris, J.B., Hunter, J.A., and Luternauer, J.L., "The bedrock surface beneath the Fraser River delta in British Columbia based on seismic measurements." Current Research 1995-E, Geological Survey of Canada, 1995, pp. 83-89.
11. Hunter, J.A., Harris, J.B., and Britton, J.R. "Compressional and shear wave interval velocity data for Quaternary sediments in the Fraser River delta from multichannel seismic reflection surveys," Geological Survey of Canada – Open File 3325.
12. Morrison, J., Quick, M.C., and Foreman, G.G. "Climate change in the Fraser River watershed: Flow and Temperature Projections," Journal of Hydrology, 263, 2002, pp 230-244.
13. Idriss, I.M. and Sun, J.I.. "SHAKE91, A computer program for conducting equivalent linear seismic response analyses of horizontally layered soil deposits" University of California, Davis, 1992.
14. Puar, S., "Seismic response of the George Massey Tunnel." University of British Columbia Department of Civil Engineering M.A.Sc. Thesis.
15. Hardy BBT Ltd. "Earthquake response of George Massey Tunnel – Geotechnical Considerations." In report to Ker, Priestman & Associates, Nov. 1989.
16. Robertson, P.K. and Wride, C.E. "Cyclic liquefactionand its evaluation based on the SPT and CPT." Proceedings of the NCEER Workshop on Evaluation of Liquefaction Resistance of Soils. Edited by Youd and Idriss, 1997.
17. Fear, C.E., and McRoberts, E.C. "Reconsideration of initiation of liquefaction in sandy soils." Journal of Geotechnical Engineering, ASCE, Vol. 121, No. 3, 1995, pp. 249-261.
18. ITASCA "FLAC - Fast langrangian analysis of continua, Version 3.4 ITASCA Consulting Group Inc., Minneapolis, Minnesota, 1996.
19. Beaty, M. 2001. A synthesized approach for estimating liquefaction-induced displacements of geotechnical structures. Ph.D. Thesis, University of British Columbia
20. Beaty, M., and Byrne, P.M. "A simulation of the Upper San Fernando dam using a synthesized approach." *In* Proceedings of Slope Stability & Landslides, 13th Annual Vancouver Geotechnical Society Symposium, 1999, pp. 63-72.
21. Puebla, H., Byrne, P.M., and Phillips, R. Analysis of CANLEX liquefaction embankments: prototype and centrifuge models. Canadian Geotechnical Journal, 34: 641-657.
22. Beaty, M., and Byrne, P.M., An effective stress model for predicting liquefaction behaviour of sand. Geotechnical Earthquake Engineering and Soil Dynamics III. P. Dakoulas, M. Yegian, and R Holtz (eds.), ASCE, Geotechnical Special Publication 75 (1): 766-777,1998.
23. Byrne, P.M., Park, S.S., Beaty, M., Sharp, M., Gonzalez, L., and Abdoun, T., Numerical modeling of liquefaction and comparison with centrifuge tests," Canadian Geotechnical Journal, 41, 2004.
24. Tokimatsu, K.A.M. and Seed, H.B. "Evaluation of Settlement of Sands Due to Earthquake Shaking, "Journal of Geot. Engineering, ASCE, Vol. 113, No. 8, pp. 861-878, 1987.
25. Adalier, K., Abdoun, T., Dobry, R., Phillips, R., Yang, D., and Naesgaard, E. "Centrifuge modeling for seismic retrofit design of an immersed tube tunnel," International Journal of Physical Modeling in Geotechnics, 3(2): 23-32. 2003.
26. Park, S.-S., and Byrne, P.M. "Stress densification and its evaluation." Canadian Geotechnical Journal., Vol. 41 (1):181-186, 2002.